UNIVERSITY OF CALIFORNIA,
IRVINE

p53 Restoration in Ovarian Carcinoma Harnessing a Genetic Aberration

THESIS

submitted in partial satisfaction of the requirements
for the degree of

MASTER OF SCIENCE

in Biomedical and Translational Science

by

Lindsey Elaine Minion

Thesis Committee:
Professor Sheldon Greenfield, Chair
Professor Peter Kaiser Irvine
Associate Professor Leslie M. Randall

2018

DEDICATION

To

my parents, Bill & Marsha Minion, and Roland Ford

I am forever grateful for your love and support. Here's to living the dream!

TABLE OF CONTENTS

	Page
LIST OF FIGURES	iv
LIST OF TABLES	v
ABSTRACT OF THE THESIS	vi
INTRODUCTION	1
MATERIALS AND METHODS	9
RESULTS	13
DISCUSSION	23
REFERENCES (OR BIBLIOGRAPHY)	26

LIST OF FIGURES

		Page
Figure 1	Frequency of p53 Mutations	2
Figure 2	Schematic Representation of p53 Activation	4
Figure 3	Frequency of p53 Mutations by Amino Acid	5
Figure 4	Conceptual Model of Pharmaceutical Reactivation	5
Figure 5	38RNW Inhibition of Cell Proliferation	7
Figure 6	TOV-112D Inhibition with Paclitaxel and 38RNW	13
Figure 7	Micrographs of SOAS-2 Cells with 38RNW	13
Figure 8	Cell density and DMSO Concentration Studies	14-15
Figure 9	Half the Maximal Inhibitory Concentration	15
Figure 10	Kinase Library Pathway Frequency	17
Figure 11	Kinase Library Z-Scores	17
Figure 12	Kinase Library Screen Examples	18-21
Figure 13	Clinical Collection and FDA-approved Library Z-Scores	22

LIST OF TABLES

		Page
Table 1	The half-inhibitor concentration, or the concentration of 38RNW	7

ABSTRACT OF THE THESIS

p53 Restoration in Ovarian Carcinoma Harnessing a Genetic Aberration

By

Lindsey Elaine Minion

Master of Science in Biomedical and Translational Science

University of California, Irvine, 2018

Professor Sheldon Greenfield, Chair

Ovarian cancer is the most fatal gynecologic malignancy. The majority of deaths are in advance staged patients with high-grade serous histology. Most patients respond to primary surgery and chemotherapy yet experience recurrent disease. Chemotherapy remains central to recurrent treatment and is rarely curative. There is an unmet clinical need for additional treatment options. Advancements in tumor biology, particularly the genetic landscape of ovarian cancer, shape current researched therapeutic targets. The genotypic characterization of this malignancy is generalized by chromosomal disarray and *p53* mutations. Mutations of *p53* are ubiquitous across cancer. These mutations are a rational target for therapeutic exploration due to the frequency in ovarian carcinoma and its dominant role in tumor suppression. Small molecule compounds, including 38RNW, have been developed that bind to mutated p53 and partially restore wild-type tumor suppressor function. This translational approach leads to the hypothesis that 38RNW would synergistically combine with other drugs to induce apoptosis in an *in-vitro* model. Herein, a high throughput robotic nano-technology platform was implored to identify synergistic combinations with 38RNW in TOV-112D ovarian cancer cells. A Luciferase-base cell proliferation assay was implored to determine inhibitor effects in a high-throughput approach. Z-scores were calculated comparing plate averages of luciferase values to individual compounds or change in half-inhibitor concentration. 38RNW demonstrated strong synergistic activity with mammalian target of rapamycin/phosphatidylinositol 3-kinase (mTOR/PI3K) and polo-like kinase 1(Plk-1) inhibitors. The lead candidates warrant further investigation. Our long-term objective is to develop p53 restoration drug combinations for ovarian cancer treatment.

INTRODUCTION

Significance

Epithelial ovarian cancer (OC) is a rare disease with a general population lifetime risk of approximately 1.37% of being diagnosed with this cancer [1]. Overall, OC represents less than 3% of all cancer diagnoses in United States women. However, in 2018, it is estimated to be the fifth most common etiology of cancer related death in women, surpassed only by cancers of breast, lung and bronchus, colon and rectum, and pancreas. Despite evolving treatment algorithms, OC continues to be the most fatal gynecologic malignancy with an estimated 14,070 deaths in 2018 in the United States alone [2-3]. Further, there has been little modulation of the survival rate, with an all-stage overall relative survival estimated at 44% [4-5].

The vague, insidious symptomatology of OC, proves a clinical challenge as the majority of patients are diagnosed at advanced stages where 5-year survival drops from 92.3% to 29.2% [6]. Currently, there is a lack of effective screening tools. Regular physical exams with a dedicated pelvic exam have been suggested as screening, however, calculations factor 10,000 exams would produce only one early OC detection in a population of asymptomatic patients [7]. Several studies have evaluated ultrasound and CA-125 in high-risk populations. Yet, even in this enriched population, screening is ineffective in detecting early stage disease, thus not impacting morbidity or mortality of this cancer [8]. Given these limitations and prognoses, there is an urgent need to develop additional therapeutic options for these patients.

Epithelial Ovarian Cancer Pathology & Genetics

Epithelial OC includes malignancies of fallopian and primary peritoneal origin given parallel tumor biology and natural history. Modern data suggests that OC often originates from the distal, fimbria portion of the fallopian tubes [9]. This finding resulted from prophylactic salpingo-oophorectomy in high-risk women identified as *BRCA* mutational carriers. Pathologist began meticulously sectioning tissue and identified occult pre-invasive lesions [10].

Histology further sub-classifies and describes the heterogeneity of this disease. OC tumors are classified by serous, mucous, clear-cell, endometrioid, and transitional cells [11]. High-grade serous (HGS) is the most common histology, accounting for 70% of epithelial OC [12].

Finally, much information has been gained in segregating OC by genetic status, further describing the heterogeneity of this cancer [13-14]. With a lack of successful treatment options, the Cancer Genome Atlas (TCGA) sought to identify therapeutic targets. Researchers comprehensively catalogued molecular aberrations of 316 high-grade serous adenocarcinoma tumors, finding *TP53* mutations in 96% and *BRCA* mutations in 20% of tumors [15].

Figure 1: Frequency of p53 mutations identified in high-grade serous ovarian tumors in the TCGA study.

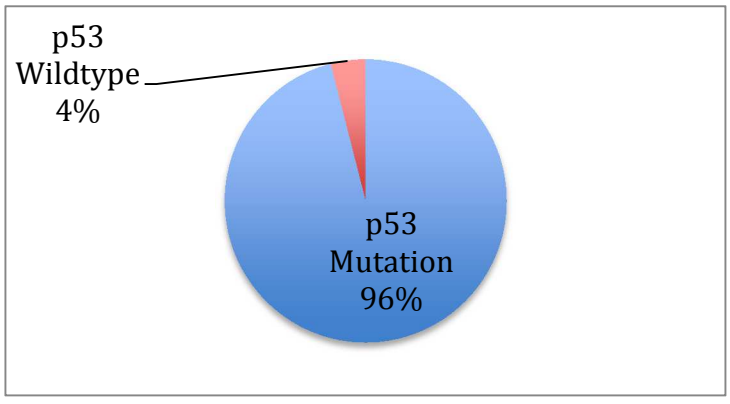

The protein produced from the *TP53* locus, p53, is a key regulatory of cell cycle, apoptosis, DNA repair, and cell senescence. In addition to ovarian cancer, *TP53* mutations occur in 40-50% of malignancies [16]. *TP53* is thus, by far, the most frequently mutated gene involved in initiation and progression of human cancer and is particularly important in OC.

Current Therapeutic Standard of Care

OC treatment utilizes two cancer therapeutic modalities: cytoreductive surgery and chemotherapy. Primary treatment paradigm includes both cytoreductive surgery and platinum-doublet chemotherapy, while recurrent disease is limited to treatment with cytotoxic chemotherapy. This template is limited by the frequency of recurrent disease, with rare curative options in that setting, despite the majority of patients achieving clinical remission with primary treatment [17-18]. The timing of recurrence, before or after six months from completion of upfront therapy, places patients into two broad categories – platinum sensitive or resistant. This designation serves to classify and determine options for treatment and demonstrate the clinical nature of this disease as patients endure through multiple lines of the chemotherapy until the tumor becomes resistant [19-20].

Historical regimens for OC have included hexamethylmelamine, cyclophosphamide, doxorubicin, and 5-fluorouracil. In the 1980's, platinum agents were introduced and dramatically increased response rates and median survival times. Gynecology Oncology Group (GOG), a corporative research organization, compared cisplatin 75 mg/m^2 plus cyclophosphamide 750 mg/m^2 every 21 days to paclitaxel 135 mg/m^2 and cisplatin 75 mg/m^2 every 21 days in GOG-protocol 111. The paclitaxel arm demonstrated an improvement to progression free survival (PFS) of 18 verses 13 months, and overall survival (OS) of 38 versus 24 months [21]. Cisplatin in combination with paclitaxel required an extending infusion of 24-hours to reduce neuropathy, thus investigators evaluated other platinum agents. In 2003, GOG conducted protocol 158 a noninferiority trial that demonstrated therapeutic equivalence between carboplatin and cisplatin. Since this trial, this chemotherapy doublet has remained the backbone of systemic, primary OC treatment [22].

Additional cytotoxic agents have been added to the armamentarium in recurrent disease. Notably, there was an 8-year period spanning from 2006 to 2014 that lacked new Food and Drug Administration (FDA) approval for OC agents. This period ended on December 19, 2014, and the poly (ADP-ribose) polymerase inhibitor (PARPi) olaparib (AZD2281) was approved by the FDA as monotherapy for recurrent OC in patients with known or suspected deleterious germline *BRCA* mutations after treatment with three or more prior lines of chemotherapy [23]. PARPi in combination with BRCA mutations produce "synthetic lethality," in which neither insult alone is fatal, but the combination results is cell death. In *BRCA*-deficient cells, single-stranded breaks are repaired in a

PARP-dependent fashion. With PARP inhibition, in these cells there is an accumulation of single-stranded breaks that are converted to double-stranded breaks for which BRCA deficiency cells cannot repair [24].

The FDA approval of olaparib is significant for several reason. As the first PARPi approved, this opened a new drug class in OC. Further, PARPi represent a targeted agent and were developed in context of *BRCA*-mutated cells [25-26]. This supports the development of other agents that harness the weakness of a genetic mutation.

P53 Cellular Functions

The ubiquitous mutation of *TP53* makes the tumor suppressor p53 a rational target for therapeutic exploration. This is due to the frequency in OC and its central role in tumor suppression. Conceptually, targeting p53 mutants for cancer therapy explores novel territory because it requires restoring the tumor suppressor function of mutated, inactive p53 protein in tumors (Fig. 2).

Figure 2: Schematic representation of p53 activation in tumor initiation, when p53, a tumor suppressor is inactivated by mutation.

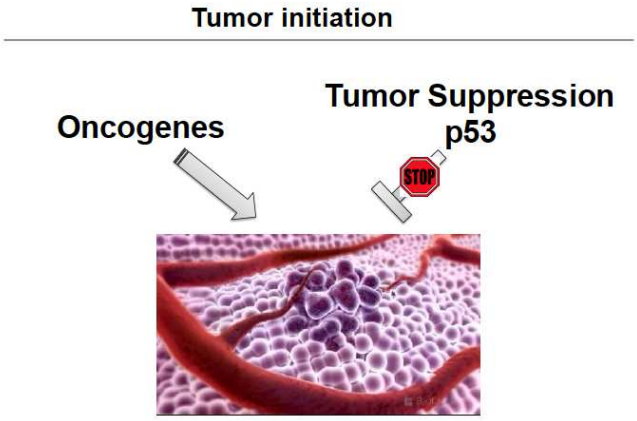

The p53 gene is located chromosome 17p13.1. This gene encodes a 292 amino acid protein transcription factor that functions within the cell cycle regulation [27]. Known as the "guardian of the genome," p53 protein exists as homo-tetramer. Each monomer with the following four domains: N-terminal transactivation domain, a proline-rich domain, a central DNA binding core domain, and a C-terminal domain that holds the tetramerization domain [27].

Functional consequences divide P53 mutations into wild-type, loss of WT function, partial loss of function, and oncomorphic [28]. The most common p53 mutations in OC include the oncomorphic missense mutations: R175, R248 and R273 [29]. In general there are six specific missense mutations found in human cancers. These are

referred to p53 hot-spot mutations (Fig. 3). These mutations are thought to change p53 conformation in a way that block p53's activity as a tumor suppressor but also leads to gain of function activities that promote tumor progression. These oncomorphic activities are likely associated with mutant p53 driving transcription of growth promoting genes that are usually not controlled by wild-type p53. Importantly, the prevalence of hot-spot p453 missense mutations results in the presence of mutant p53 protein in these cancers. This suggests that compounds can be developed that induce conformational change in mutant p53 proteins to restore tumor suppressor function and revert oncomorphic activities (Fig.4) [30].

Figure 3: The frequency of p53 mutations by amino acid in human cancer. There are 6 common or "hot-spot" mutations in DNA binding domain. Investigation drugs aimed at p53 reactivation target these mutations.

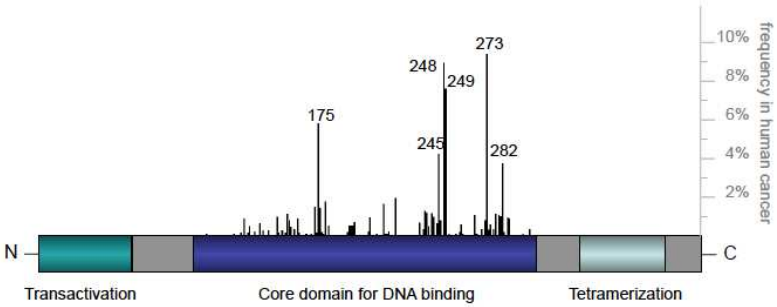

Figure 4: Conceptual model of pharmaceutical reactivation of p53 cancer mutants. Small molecule p53-reactivators like, 38RNW, would bind cancer mutated p53, restore structure and function of p53 leading cell cycle arrest, apoptosis, senescence and other p53 functions.

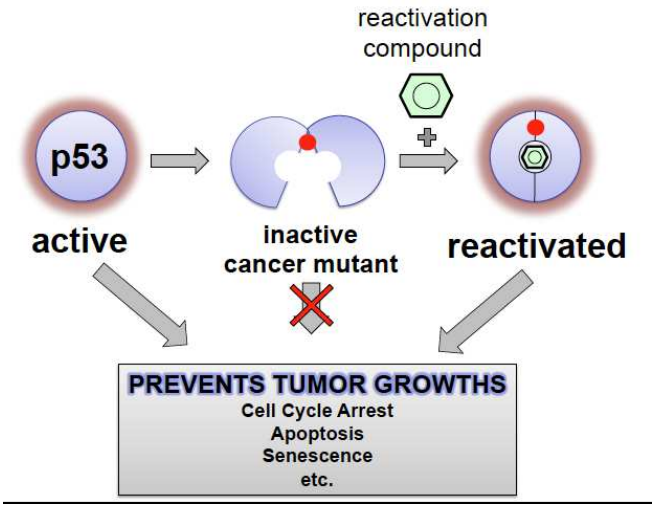

APR-246

Currently, one p53 small molecule reactivator is in clinical development. APR-246 (PRIMA-1MET) is the methylated form of APR-017 (PRIMA-1), 2,2-bis(hydroxymethyl)-1- azabicyclo[2,2,2]octan-3-one. The name PRIMA coined from p53 reactivation and induction of massive apoptosis. Researchers interrogated the National Cancer Institute (NCI) Development Therapeutics Program drug screen for small molecules that restore DNA specific binding which is an activation of mutant p53. This study screen candidate compounds by monitoring cellular growth to Saos-s-His-273 cells carrying a tetracycline-regulated mutant p53 (Tet-Off). Additional cell lines including: SKOV-His-125, SKOV-His-273 and H1299-His-175 demonstrated cell growth inhibition [31].

First-in-human trial completed in adult patients with any hematologic malignancy or hormone-refractory metastatic prostate carcinoma (n=22). This population was not enriched, as therapeutic response was not a primary outcome, therefore patients were included regardless of TP53 mutational status. As a phase-one study, the primary objects were safety, pharmacokinetics, and establishing the dose-limiting toxicities (DLTs) of APR-246. [32].

38RNW Test Compound (NSC319726)

In 2012, an attempt was made to identify modulators of p53. One group utilized the NCI anticancer drug screen data (48,129 compounds) in sixty human cancer cell lines. This project identified candidate NSC319726 or 38RNW. This compounds is a member of the thiosemicarbazone group. Confirmation specific antibodies by immunofluorescence demonstrated that NSC319726 produces a conformational change in the $p53^{R175}$ mutant [33-34]. The Kaiser laboratory independently identified a number of diverse small molecules that reactivate p53 hot-spot mutations. Among them was a derivative of NSC319726, 38RNW (unpublished data). This molecule was shown to bind mutant forms of p53 in-vitro in a purified biochemical system and restore function to p53 in cells (unpublished data).

The therapeutic window of 38RNW is ideal for testing (Table 1, Fig. 5). Our laboratory-demonstrated activity across p53 mutational sites, further supports development that can be implored across several p53 mutations. The compound was selected for its known effects and availability.

Table 1: The half-inhibitor concentration, or the concentration of 38RNW to induce a 50% reduction in cell number (nM= nano molar).

p53 hotspot cancer allele	IC50
R175H	4-12 nM
G245S	10-20 nM
R249S	15-30 nM
R282W	30-100 nM
Y220C	50-150 nM
R248W	200-300 nM
R273H	300-500 nM

Figure 5: Inhibition of cell proliferation by 38RNW depends on p53 mutants

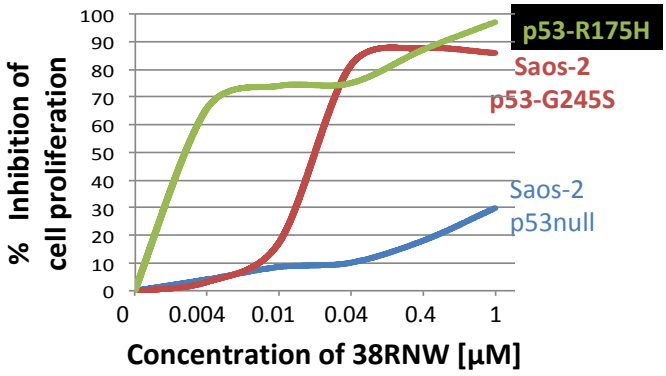

Study Aim

This study explores synergy between p53 reactivation and drugs that are either currently used or are considered for use in treatment of ovarian cancer. The hypothesis for this work is that we can identify drug combinations with the p53 reactivation compound 38RNW that act synergistically and therefore increase efficacy in cancer cell killing. While p53 reactivation is a conceptually novel approach for ovarian cancer therapy, it is possible that FDA-approved drugs that are currently not considered for treatment of ovarian cancer show strong synergistic effects when combined with p53 reactivation compounds. Therefore, a high throughput robotic nano-

technology screening was preformed to identify compounds that act synergistically with the p53 reactivator 38RNW. Our long-term objective is to explore synergy of p53 restoration with FDA-approved drugs for effective treatment of OC.

MATERIALS AND METHODS

Cells

TOV-112D (her2/neu+, $p53^{R175H}$) cells were derived from American Type Culture Collection (ATCC) and were documented to be mycoplasma free. This cell line was selected because TOV112D cells grow easily in multi-well formats and show a very consistent response to the p53 reactivation compound 38RNW. Cells were grown and expanded in media composed of a 1:1 mixture of MCDB 105 medium containing a final concentration of 1.5 g/L sodium bicarbonate and Medium 199 containing a final concentration of 2.2 g/L sodium bicarbonate, 15% of fetal bovine serum and 5% penicillin-streptomycin antibiotics. Cells were maintained at 37 degrees Celsius temperature, 5% CO_2 in cell culture flasks with 10 mL of media. Standard cell culture technique to expand cells required high thoughput experimentation.

Compounds

Chemical libraries were prepared by the Molecular Shared Screening Resource core facility at the University of California, Los Angeles. The small molecule compound libraries included the Kinase Library (430 compounds), the National Institute of Health (NIH) I and II Clinical Collection (725 compounds), and FDA-approved drug library (1200 compounds). The rationale for the FDA-approved drug library is to determine secondary indications and expedite approval. Compounds included have structural diversity, known safety profiles, and bioavailability in humans. The NIH I and II Clinical Collection compounds do not have toxicological liabilities as previously implored in clinical test, yet they are without FDA labels and thus facilitate transition into clinic. The rationale for testing the Kinase Library is that these compounds target known signaling pathways and synergy with p53 reactivation and can identify signaling pathways that, when inhibited in ovarian cancer, generate a synthetic lethal effect with p53 reactivation.

The cell-based assay execution in a 386-well format using the robotics setup available at the MSSR center. The screen is based on a constant sublethal dose of 38RNW (0.9 nM), IC 20 and a dose range of library compounds.

Equipment

A nano-technology platform including automated, robotic equipment for cell culture and compound transferred was used throughout the study. We utilized the Multidrop/MultiFlo FX for contact free, liquid dispenser for media and cell transfer. The Biomek FX platform performed library drug transfer using precision machine slotted pins. Luminescence readout of CellTiter Glo was achieved with the Perkin Elmer Envision.

Preliminary Studies

To determine optimal drug screening conditions, several test parameters were evaluated prior to drug screening including cell density and a dose response curve of TOV-112D cells with test compound 38RNW. Additionally, the toxicity of the test compound vehicle, dimethyl sulfoxide (DMSO), was investigated to TOV112D tolerance.

Cells were collected from growing stock by tripsinizing cells and diluting in media. Cells per mL were calculated. The liquid handler with increasing density per well transferred cells and media into wells. Cells were plated on a 384-well plate with increasing cell density ranging from 500 cells per well to 3,000 cells per well by increments of 500 cells per well. DMSO at x2 concentration from final was added to wells. The following concentrations were studied: 0, 0.5, 1.0, 1.5, 2.0, 2.5, and 3%. Each DMSO concentration was tested throughout the range of cell density. After a 72-hour incubation, Hoechst 33342 stain was added to well to label cells. Staining buffer diluted in cell culture media, with a final concentration of 1 ug/ml of Hoechst 33342. Cells were incubated for 10 minutes at 37 degrees. Wells were imaged with fluorescence microscope with appropriate filters. Concentration of DMSO and cells per well to achieve 80% confluent was visually determined.

Next, a dose response curve was determined for 38RNW in 3,000 cells per well, with a 0.5% DMSO concentration. Increasing concentrations of 38RNW were added to 384-well plate with 25 uL of media and compound per well. Compound in media was plated using the automatic liquid handler. Cells were collected using standard cell culture technique. Cells concentration per mL was calculated; the ratio of cells to media was added to obtain 3,000 cells in 25 uL. Cells and media were plated using the automatic liquid handler. After a 72-hour incubation, a cell viability assay was conducted. The CellTiter-Glo Luminescent reagent was added to each well

with the automatic liquid handler (25 uL per well). After a 10-minute incubation, plates were read. Cell viability verses 38RNW concentration was graphed. The IC50 and IC20 or 50% and 20% inhibitor concentration was calculated. This is the dose of 38RNW in which half or 20% of the cells are expected to die.

Library Screen

From preliminary studies, library screen utilized 0.9 nM concentration of 38RNW in 3,000 cells per well, with a final concentration of 0.5% DMSO. Standard cell culture was implored throughout screening. 25 uL of media was added to 384-well plates using the automatic liquid handler. Libraries were transferred into wells utilizing the Biomek FX platform. The NIH I and II Clinical Collection and FDA-approved drug library studies were conducted at one concentration as determined by the library. The Kinase Library was conducted at 9 different concentrations.

Cells were collected using standard cell culture technique. Cells concentration per mL was calculated; the ratio of cells to media was added to obtain 3,000 cells in 25 uL. Cells and media were plated using the automatic liquid handler. After a 72-hour incubation, a cell viability assay was conducted. The CellTiter-Glo Luminescent reagent was added to each well with the automatic liquid handler (25 uL per well). After a 60-minute incubation, plates were read. Cell viability verses 38RNW concentration was graphed and IC20 was calculated.

Analysis

Our independent variable was the addition of 38RNW to TOV-112D cells exposed to the Kinase, NIH I and II Clinical Collection and FDA-approved drug libraries. The dependent variable for the NIH I and II Clinical Collection and FDA-approved drug library studies were calculated Z-scores. Raw cell viability data was averaged per plate, and wells were compared to this average producing a Z-score. The threshold to be considered a hit was a preset Z-score of 3 or greater.

Multiple doses of each kinase inhibitor were tested with one concentration of 38RNW and without 38RNW. Dose-response curves were calculated for the Kinase Library. The dependent variable, or threshold to be considered a hit, was a modulation of the IC50. Z-scores were calculated based on the change in IC50 with and

without 38RNW. Additionally, analysis for this library screen was determined qualitative assessment of the IC50 curves by the investigator.

Enrichment scores and significance of kinase library hits were determined using a Fisher's Exact Test.

RESULTS

Preliminary Studies

To explore proof of concept experiments, we tested the effect of combinations between p53 reactivation with 38RNW and paclitaxel. (Fig. 6). Four different concentrations of 38RNW were combined with six different doses of paclitaxel and inhibition of TOV-112D cells. The compound was selected for its known effects and availability. Work in our laboratory demonstrates that 38RNW induces sensitivity to paclitaxel, a standard chemotherapy used in ovarian cancer

Figure. 6: Survival of TOV-112D ovarian cancer cells after 3 days treatment with paclitaxel and the p53 reactivator 38RNW. A dose-dependent 38RNW inhibition of cell proliferation was demonstrated on TOV-112D cells

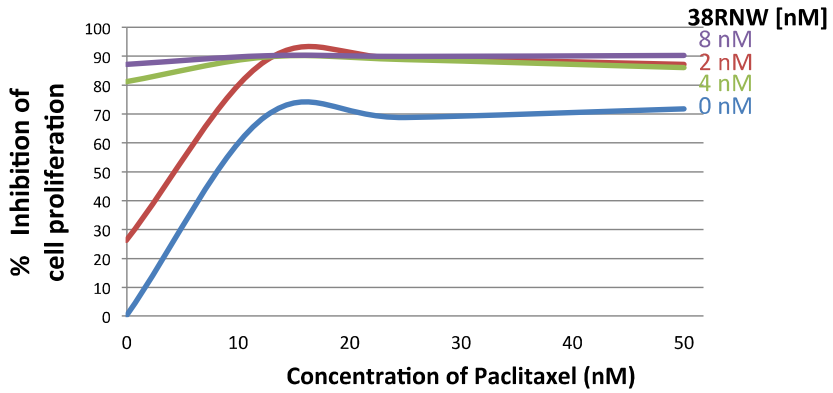

Figure 7: Micrographs of engineered SOAS-2 cells carrying G245S and R175H p53 mutations. These cell lines were incubated with DMSO or 38RNW for 12 hours. The following micrographs demonstrate cellular apoptosis induced with 38RNW exposure.

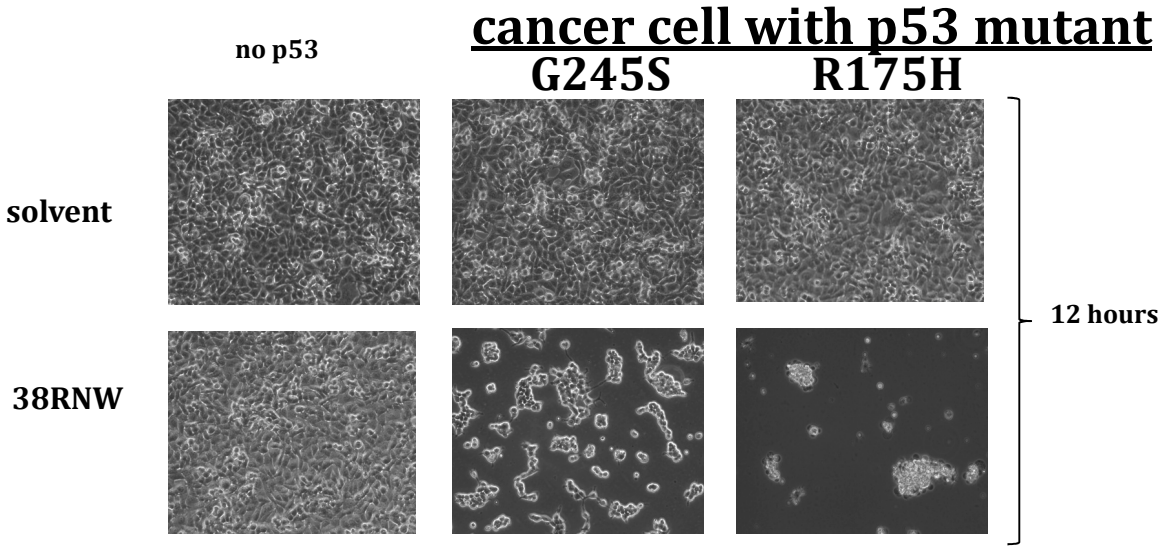

Optimization of IC50 for 38RNW in the 386-well High Throughput Format

Cell density was initially optimized for TOV 112D cells in the 384 well format used in the compound screening campaign. The next step was to explore DMSO tolerance of TOV 112 cells. Because all screening compounds are dissolved in DMSO, it was important to test sensitivity to the solvent. This test revealed that DMS concentrations in screening wells should not be higher than 0.5% to avoid solvent inhibition of TOV 112 cells (Fig. 8). Screening conditions used DMSO concentrations lower than .5%.

Figure 8: Preliminary study of cell density and DMSO concentration, to determine parameters for future experiment. Cells were plated on a 384-well plate with increasing cell density ranging from 500 cells per well to 3,000 cells per well by increments of 500 cells per well. This plate was incubated for 72-hours. After incubation, DMSO at x2 concentration from final was added to wells. The following concentrations were studied: 0, 0.5, 1.0, 1.5, 2.0, 2.5, and 3%. Each DMSO concentration was tested throughout the range of cell density. After a 72-hour incubation, Hoechst 33342 stain was added to well to label cells. Below are the Hoechst 33342 stained images.

A. Cell density of 3,000 cells per well of TOV-112D without DMSO after 72-hour incubation.

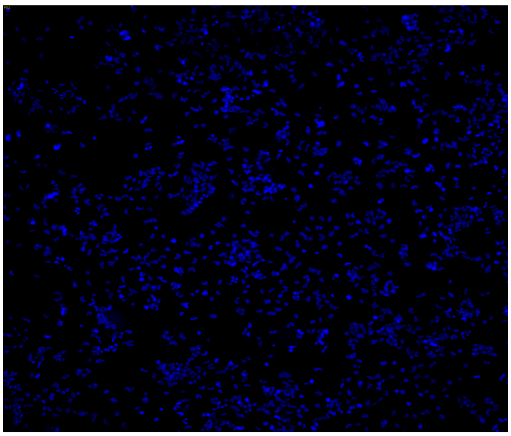

B. Cell density of 3,000 cells per well of TOV-112D with 0.5% DMSO after 72-hour incubation. Of note this DMSO concentration and, cell density were the parameters for future experiments.

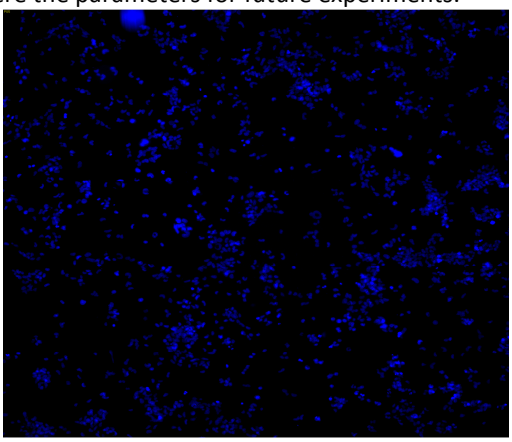

C. Cell density of 3,000 cells per well of TOV-112D with 3% DMSO after 72-hour incubation.

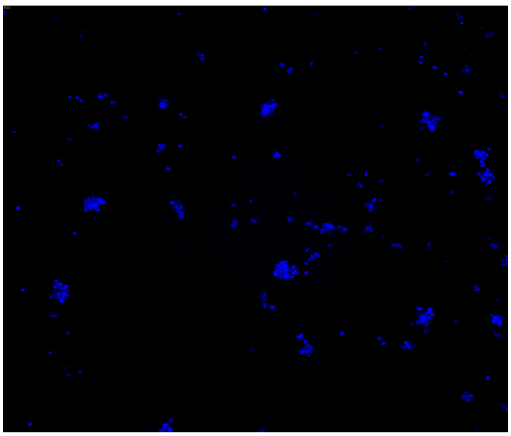

The synergy screen was planned to utilize a low inhibitory dose of 38RNW. We aimed at an inhibitory concentration that would reduce cell proliferation by 10-20%. To this end, we generated a very detailed dose response curve in the screening format. We noticed that the dose response curve is very steep and biphasic in the higher dose concentrations. However, behavior of the dose response curve at the relevant lower inhibition concentration was very good and we could determine 0.9nM as our screening concentration. At this concentration, we consistently observe between 10 and 20% inhibition of TOV-112D cell proliferation.

Figure 9: Graph depicting half the maximal inhibitory concentration (IC50). From this preliminary experiment, IC20 (0.9 nM concentration) of 38RNW was selected for library screen. Y-axis: relative number of cells after 72-hours treatment with compounds concentrations as indicated on the X-axis. Highest concentration was 500nM and a 2-fold dilution series of the compound was used.

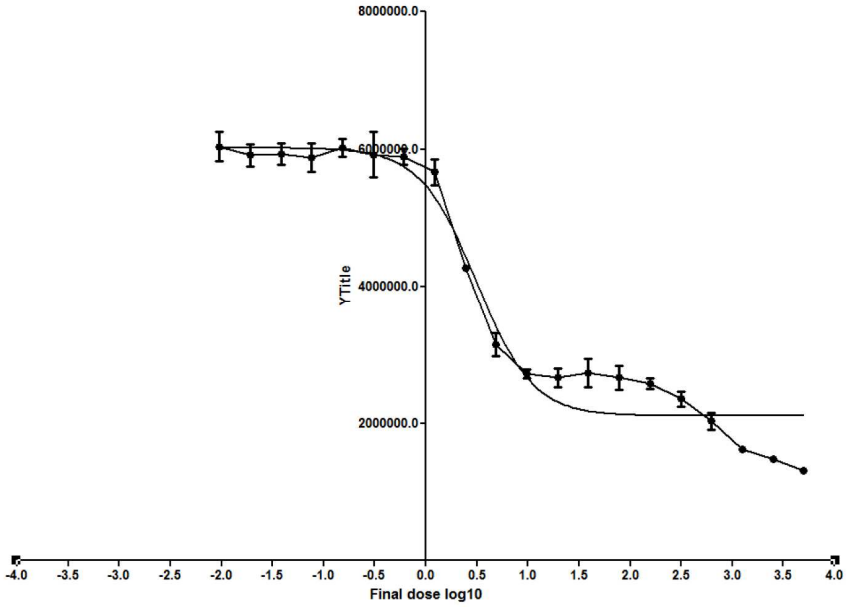

Nano-Technology High-Throughput Robotic Screen

We screened two separate library sets. (1) Kinase Inhibitor Library (430 compounds). This library was screened in a dose response series. (2) Clinical compounds: This set contains the FDA-approved drug library (1200 compounds), the Clinical collections I + II (725 compounds that failed in clinical trials, "repurposed drugs") and the Drugable Compound Set (8000 compounds). The clinical set was screened in a single dose approach.

The screening was notable for 75 primary hits in the 2,355 total compounds screened. The overall screen hit rate was 3%.

Kinase Library Screen

The primary screen resulted in 34 hits based on Z-score cut off -3. After manual inspection of the dose response curves, 10 of these compounds were determined not likely to be of significance based on an atypical linear dose response curve or termination of inhibitory effects at 50%. Inspection of the remaining 24 hits showed a distribution of inhibitors (Fig. 10). Of 430 compounds, 49 and 6 are in the rapamycin/phosphatidylinositol 3-kinase (mTOR/PI3K), and polo-like kinase 1(PLK) pathways, respectively. Twelve of 49 mTOR/PI3K pathway compounds met inclusion criteria and are considered a hit. Five of 6 of the Plk-1 pathway compounds met inclusion criteria, and are considered a hit. These are remarkable findings and are further confirmed by statistical analysis of enrichment using the Fisher's Exact Test, which provides p values of 1.243×10^{-6} and 2.028×10^{-6} for mTOR/PI3K and Plk-1 pathway inhibition hits, respectively. The remaining 7 hits were of the following pathways and may be interesting but need further evaluation: 1 cyclin-dependent kinase (CDK), 1 mitogen-activated protein kinase (MEK), 1 serine/threonine-protein kinase (PAK), 1 tyrosine kinase (Bcr-Abl), 1 Aurora Kinase, 1 epidermal growth factor receptor (EGFR) and 1 glycogen synthase kinase (GSK-3).

Figure 10. Kinase library screen hits were of the following pathways: 12 mammalian target of rapamycin/phosphatidylinositol 3-kinase (mTOR/PI3K), 5 polo-like kinase 1(Plk-1), 1 cyclin-dependent kinase (CDK), 1 mitogen-activated protein kinase (MEK), 1 serine/threonine-protein kinase (PAK), 1 tyrosine kinase (Bcr-Abl), 1 Aurora Kinase, 1 epidermal growth factor receptor (EGFR) and 1 glycogen synthase kinase (GSK-3).

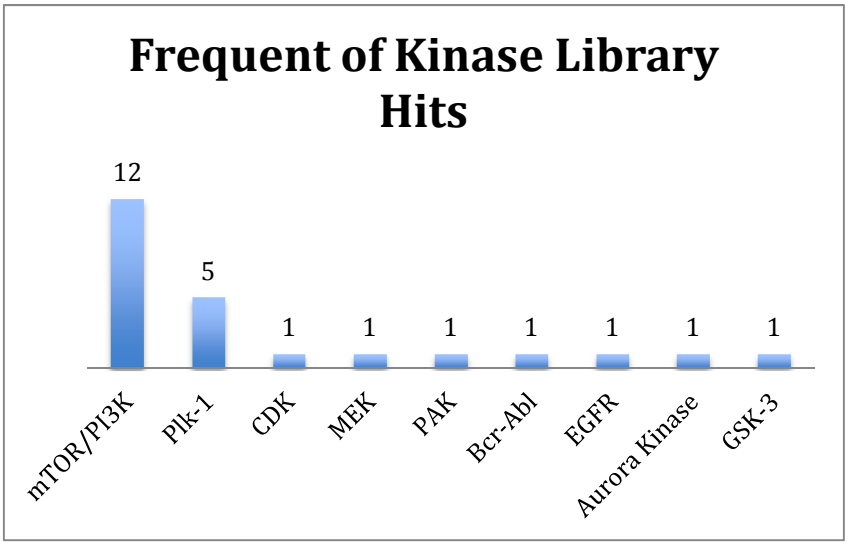

Figure 11: Graph of z-scores of 430 compound combinations results from the Kinase library. Z-scores were calculated from the change in IC50. Twenty-four compounds had a score that met inclusion criteria of greater than 3, which represents 3-standard deviation from the average cell viability.

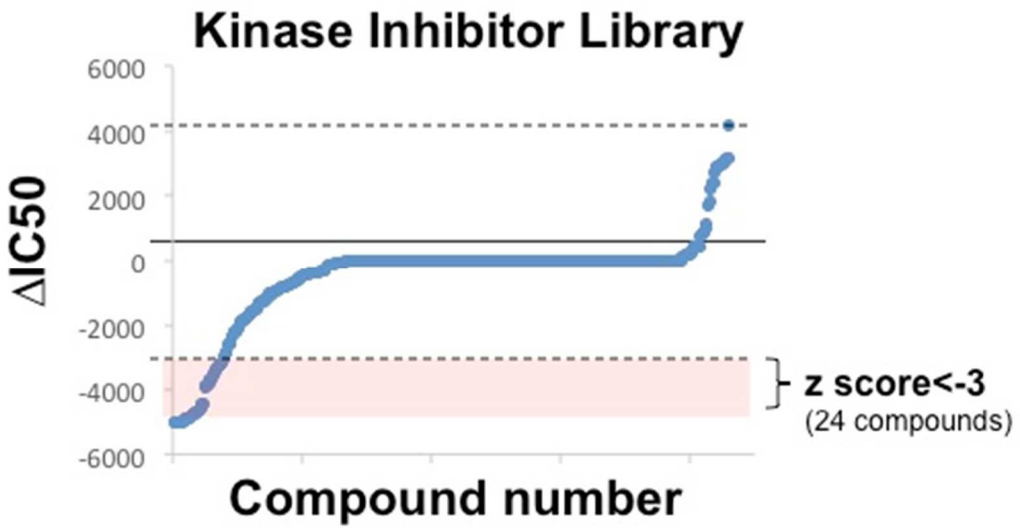

Representatives of some of the most interesting classes of kinase inhibitors are displayed with their dose response curves in Figure 12. We find a remarkable synergy, often moving inhibitory concentrations for kinase inhibitors by more than 3 orders of magnitude by addition of low dose p53 reactivator 38RNW.

Figure 12: Selected graphs from kinase library screen. IC50 curves with and without 38RNW

A.

PLK1 Kinase Inhibitor
GSK461364

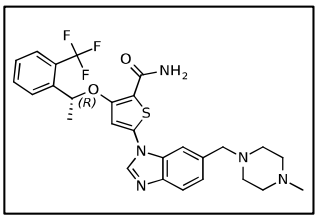

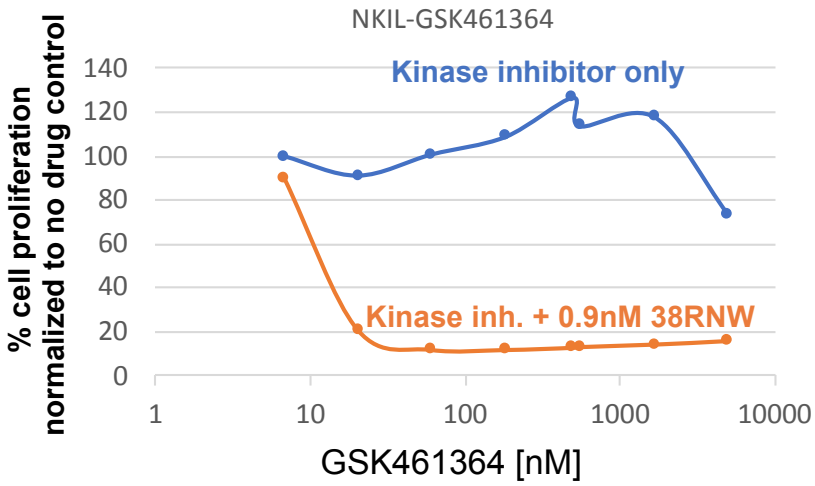

B

mTOR Kinase Inhibitor
WYE-132

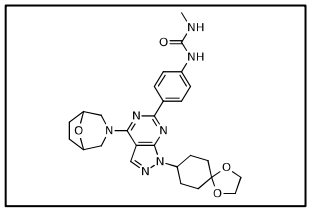

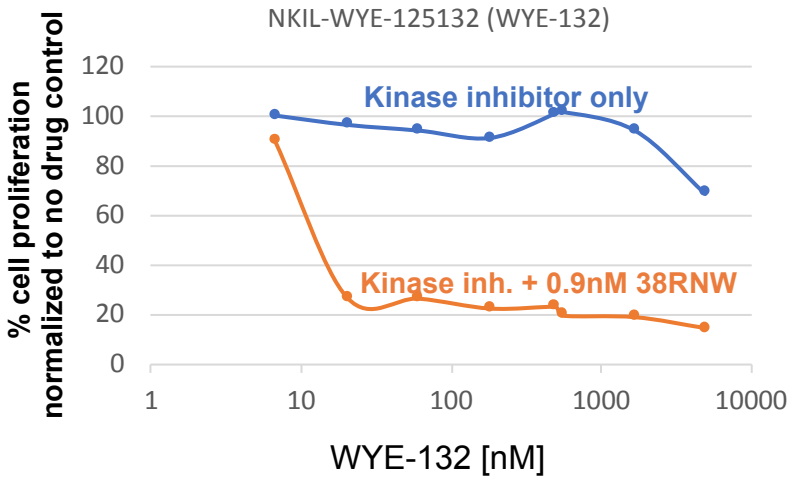

C

CDK Inhibitor (1,2,5,9)
Dinaciclib

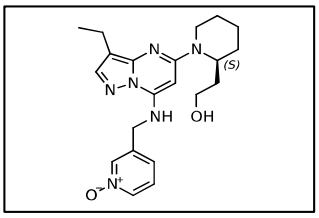

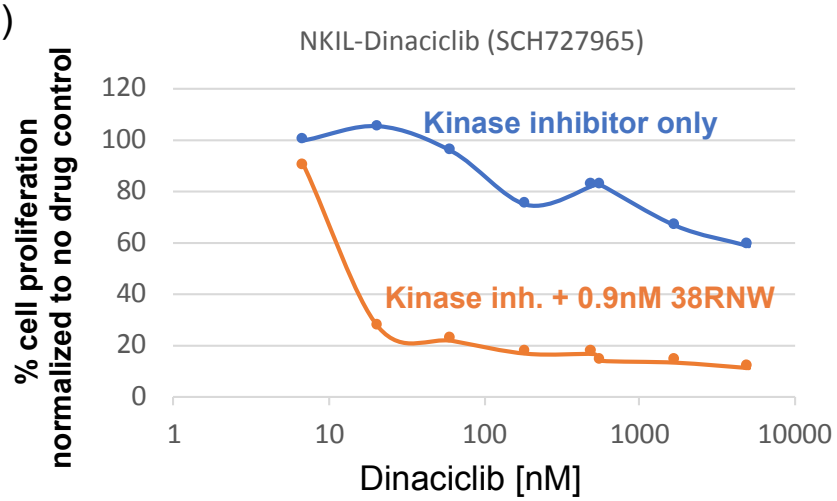

D.

PI3 Kinase Inhibitor
BGT226

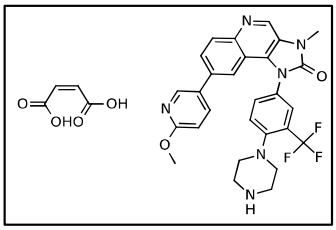

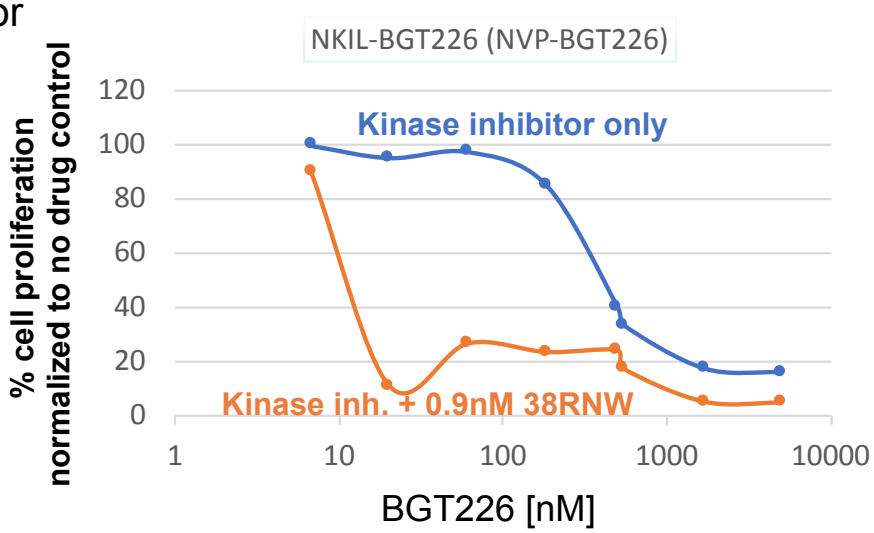

E.

Aurora Kinase Inhibitor
MK-8745

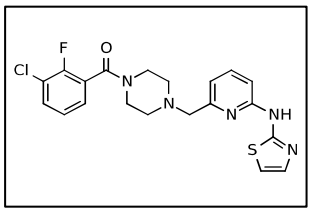

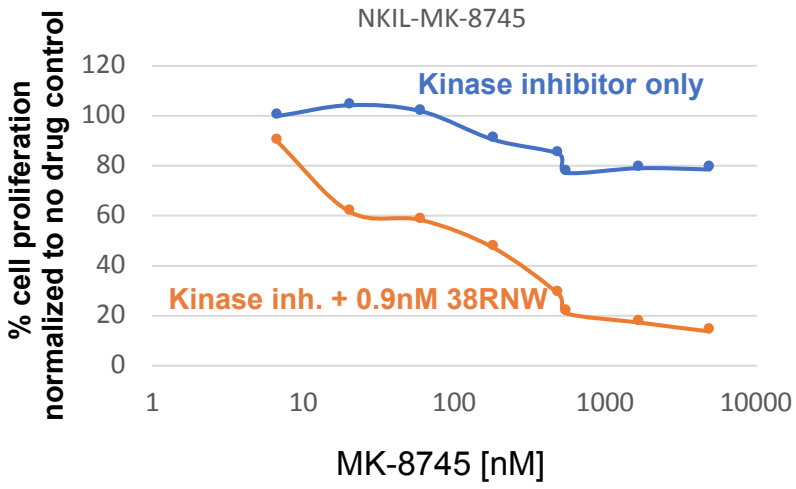

Clinical Compound Screen

Within the 41- NIH I and II Clinical Collection and FDA-approved drug library hits with Z-scores greater than 3. Of note, two compounds had Z-scores of greater than 7: prochlorperzaine maleate and methotrexate monohydrate. Paclitaxel, which served as our initial proof-of-concept model compound, was also identified in this unbiased screen. It is also of note that many compounds showed significant higher synergy with 38RNW than paclitaxel. Interestingly, there were 4 topoisomerase inhibitors among the hits. This suggests that this class of compounds should be further investigated for synergy with p53 reactivation.

Figure 13: Graph of z-scores of 1,925 compound combinations results from the NIH I and II Clinical Collection and FDA-approved drug library. Forty-one compounds had a score that met inclusion criteria of greater than 3, which represents 3-standard deviation from the average cell viability.

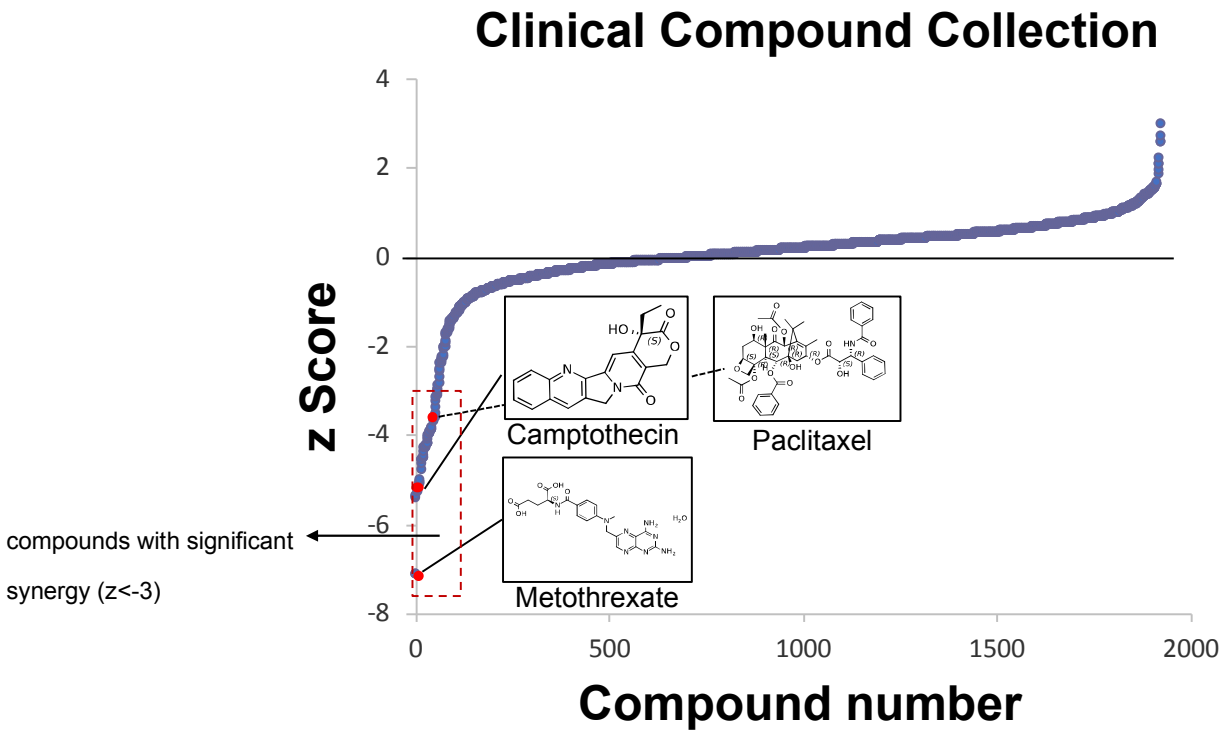

DISCUSSION

Reactivation of the body's tumor suppressing activity by drugs that restore activity to mutated, inactive forms of the tumor suppressor p53 is a novel therapeutic strategy for cancer. In contrast to other targeted therapies which inhibit tumor growth promoting pathways, we, and others, pursue a novel concept to restore the body's own defense mechanism against cancer. It is expected that p53 reactivation drugs will soon reach the clinic. It is therefore important to test synergistic effects with other therapeutics to ensure success during the translational stages. The high prevalence of p53 mutations as drivers of ovarian cancer make this deadly cancer exceptionally suited for the proposed research.

Compounds producing interesting synergistic effects will then be evaluated in more detailed dose response studies and animal models. The lead candidates we have identified in combination with 38RNW include inhibitors of the mTOR/PIK3 and Plk-1 pathways. p53 effects are multifaceted, as this protein binds to 4,000 sites and regulates transcription of 500 genes, therefore has countless downstream effects that are not fully characterized at this point [35]. Well known are those of cell cycle, however p53 can more accurate be described as a responder of cellular stress including events of starvation or oxidative stress [35].

The PI3K/AKT/mTOR pathway functions in the protection ovarian follicle from environmental insults by promoting cell survival [36]. In ovarian malignancy, the exact mechanisms are less clear, however about a third of ovarian cancer will contain an aberration to this pathway. Aberrations, including mutations or amplification, of the PI3K/AKT/mTOR pathway were seen in 34% of ovarian tumors studied in the TCGA [15]. Activation of this pathway results in proliferation and invasion [36]. Further, activation of mTOR signaling has been showed to be an adverse prognostic factor for ovarian cancer [37].

Given the biological rationale and strong pre-clinical data, the GOG studied the mTOR inhibitor temsirolimus in a phase II trial in patients with persistent or recurrent ovarian cancer. Of the 54 evaluable, unselected patients, 9.3% (n=5) demonstrated a partial response (90% CI, 3.7-23.4%), 24% had a PFS of greater than 6 months (90% CI, 14.89-38.6%). In this study population, median PFS and OS were 3.2 and 11.6 months, respectively [38]. This modest activity was met with several Grade 3 and 4 events. The most common of which included fatigue (n=4) and gastrointestinal events (n=6). Based on this study data, the authors concluded

temsirolimus did not warrant phase III investigation as a single agent. Of noted, the longest responder in this study received 24 cycles, and a PFS at 21 months was a longer duration than the median study OS of 11.6. This study population was unselected with no information on *p53*, nor PI3K/AKT/mTOR pathway mutation status.

Polo-like kinases (Plk) have similar functions of p53 and regulate checkpoint controls and multiple events within mitosis [39]. There are four identified kinase is this family named Plk1-4, of which Plk-1 is well described [38]. Several malignancies, including ovarian cancer, demonstrate overexpression of Plk1 [40]. Analyzing tissue samples from (n=116) patients with ovarian pathology from benign cystadenoma to borderline tumors to invasive carcinoma and correlating PLK1/3 expression to clinical history demonstrated a coloration with expression and patient prognosis [41]. Patients with tumors expressing Plk1 had a reduced OS on univariate ($p=0.02$) and multivariate analysis (p-0.03). Further, ovarian cancer Plk expression is correlated with high grade ($p<0.001$) and increased expression with higher stage of disease ($p<0.001$) [42].

Intersecting with our test compound and p53 reactivity, in-vitro investigations demonstrate Plk-1 functions in cell cycle via p53. Experiments conducted with Plk-1 depleted HeLa cells, Western blots detected increase of the stability of p53 in depleted cells, suggesting that Plk-1 inhibition would effect cell cycle via a p53 dependent pathway [40].

Plk-1 inhibitors have entered clinical testing. Phase I investigation of Plk-1 inhibitor ON 01910.Na, of the 20 patients enrolled, one subject with ovarian cancer demonstrated an objective response. This participant had platinum refractory disease that progressed on upfront carboplatin paclitaxel and did not response to second line topotecan. After cycle four, this participant had a documented partial response and remained progression free for 24 months. This activity is encouraging given the low response rate in the platinum-refractory population [43].

This study has several limitations. To date, we have only tested this screen in one ovarian cancer cell line; expansion to other cell lines would support our findings. TOV-112D cell line was obtained from a 42-year-old female with Stage IIIC, primary endometrioid adenocarcinoma. The oncogene profile includes her2/neu+, mutated p53 at 175 Arg->His. Given that our test compound is a p53 activator, we hypothesis that other p53 mutations of the DNA binding site would synergistically combine with inhibitors of the mTOR/PIK3 and Plk-1 pathways in ovarian cancer *in-vivo*. However, this is unproved at this juncture.

Therapeutic investigation of novel agents involves a progressive experimental plan from *in-vitro*, animal, and, finally, human subjects. Preclinical experiments establish antiproliferative activity, confirm proof-of-concept, and validate the use in animal models. Cell line investigations remain a central starting point for therapeutic development. Here, we completed a portion of *in-vitro* testing and identified therapeutic combinations for further investigation. Next immediate steps include validation of activity in high-grade ovarian cancer cell lines with the most common p53 mutations. If data confirms and activity demonstrates, then murine model testing would be considered.

In conclusion, epithelial ovarian cancer continues to remain an unmet need with an unacceptable mortality. Further treatments need to address the biologic heterogeneity elucidated in modern ovarian cancer studies. Given the frequency of *p53* mutations in high-grade serous epithelial ovarian cancer, p53 reactivation remains an attractive mechanism not currently harnessed in clinical care. Candidate combinations display synergistic activity in ovarian cancer cells in this *in-vitro* study. The findings presented demonstrate strong scientific rationale and warrant continued pre-clinical investigation.

REFERENCES

1. Pearce CL, Stram DO, Ness RB, et al. Population distribution of lifetime risk of ovarian cancer in the United States. Cancer Epidemiol Biomarkers Prev. 2015 Apr;24(4):671-676.
2. American Cancer Society, 2018 Facts and Figures. https://www.cancer.org/content/dam/cancer-org/research/cancer-facts-and-statistics/annual-cancer-facts-and-figures/2018/cancer-facts-and-figures-2018.pdf
3. Coleman RL, Monk BJ, Sood AK, et al. Latest research and clinical treatment of advanced-stage epithelial ovarian cancer. Nat Rev Clin Oncol. 2013 Apr;10(4):211-24.
4. Baldwin LA, Huang B, Miller RW, et al. Ten-year relative survival for epithelial ovarian cancer. Obstet Gynecol. 2012 Sept;120(3):612-8.
5. Chan JK, Cheung MK, Husain A, et al. Patterns and progress in ovarian cancer over 14 years. Obstet Gynecol. 2006 Sep;108(3 Pt 1):521-8.
6. Cancer Stat facts: ovarian cancer. https://seer.cancer.gov/statfacts/html/ovary.html. Accessed 8/19/2018.
7. Di Saia, Philip, et al. *Clinical Gynecologic Oncology.* Philadelphia, PA, 2007. Print.
8. Woodward ER, Sieightholme HV, Considine AM, et al. Annual surveillance by CA125 and transvaginal ultrasound for ovarian cancer in both high-risk and population risk women is ineffective. BJOG. 2007 Dec;114(12):1500-9.
9. Piek JMJ, Verheijen RHM, Keneman P, et al. BRCA1/2-related ovarian cancers are of tubal origin: a hypothesis. Gynecol Oncol. 2003 Aug;90(2):491.
10. Nik NN, Vang R, Shih IeM, Kurman RJ. Origin and pathogenesis of pelvic (ovarian, tubal and primary peritoneal) serous carcinoma. Annu Rev Pathol. 2014;9:27-45.
11. Gilks CB, Prat J. Ovarian carcinoma pathology and genetics: recent advances. Hum Pathol. 2009 Sep;40(9):1213-23.
12. Seidman JD, et al. The histologic type and stage distribution of ovarian carcinomas of surface epithelial origin. Int. J. Gynecol. Pathol. 23, 41-44 (2004).
13. Prat J, New insights into ovarian cancer pathology, Ann. Oncol. 23 (Suppl. 10) (2012) 111–117.
14. Randall LM, Pothuri B, Swisher EM, et al. Multi-disciplinary summit on genetics services for women with gynecologic cancers: A Society of Gynecologic Oncology White Paper. Gynecol Oncol. 2017 Aug;146(2):217-224.
15. Cancer Genome Atlas Research Network. Integrated genomic analyses of ovarian carcinoma. Nature. 2011 Jun 29;474(7353): 609-15.
16. Kandoth, C. et al. Mutational landscape and significance across 12 major cancer types. Nature 502, 333-339, doi:10.1038/nature12634 (2013).
17. Naumann RW, Coleman RL. Management strategies for recurrent platinum-resistance ovarian cancer. Drugs. 2011 Jul 30;71(11):1397-412.
18. Herzog TJ. The current treatment of recurrent ovarian cancer. Curr Oncol Rep. 2006 Nov;8(6):448-54.
19. Markman M, Rothman R, Hakes T, et al. Second-line platinum therapy in patients with ovarian cancer previously treated with cisplatin. J Clin Oncol 1991 Mar;9(3):389-93.

20. Banerjee S, Kaye SB. New Strategies in the treatment of ovarian cancer: current clinical perspectives, and future potential. Clin Cancer Res. 2013 Mar 1;19(5):961-8.
21. McGuire III WP, Hoskins WJ, Brady MF, et al. A Phase III Randomized Study of Cyclophosphamide and Cisplatin versus Paclitaxel and Cisplatin in Patients with Suboptimal Stage III and IV Epithelial Ovarian Cancer. N Engl J Med 334: 1-6, 1996.
22. Ozols R, Bundy BN, Greer BE. Phase III trial of carboplatin and paclitaxel compared with cisplatin and paclitaxel in patients with optimally resected stage III ovarian cancer: a Gynecologic Oncology Group study. J Clin Oncol 21(17): 3194-200, 2003.
23. http://www.onclive.com/web-exclusives/fda-grants-maintenance-olaparib-priority-review-for-ovarian-cancer. Accessed 7/11/2017.
24. Lord CJ, Ashworth A. PARP inhibitors: Synthetic lethality in the clinic. Science. 2017 Mar 17;355(633):1152-1158.
25. Farmer H, McCabe N, Lord CJ, et al. Targeting the DNA repair defects in BRCA mutant cells as a therapeutic strategy. Nature. 2005 Apr 14;434(7035):917-21.
26. Bryant HE, Schultz N, Thomas HD, et al. Specific killing of BRCA2-deficient tumours with inhibitors of poly(ADP-ribose) polymerase. Nature. 2005 Apr 14;434(7035):913-7.
27. Saha T, Kar RK, Sa G. Structural and sequential context of p53: A review of experimental and theoretical evidence. Prog Biophys Mol Biol. 2015 Mar;117(2-3):250-263.
28. Brachova P, Thiel KW, Leslie KK. The consequence of oncomorphic *TP53* mutations in ovarian cancer. Int J Mol Sci. 2013 Sep 23;14(9):19257-75.
29. P53 mutation in ovarian cancer. http://p53.free.fr/Database/p53_cancer/p53_ovary.html. Accessed July 30, 2016.
30. Yue X, Zhao Y, Xu Y, et al. Mutant p53 in cancer: accumulation, gain-of-function, and therapy. J Mol Biol. 2017 Jun 2;429(11):1595-1606.
31. Bykov VJN, Issaeva N, Shilov A, et al. Restoration of the tumor suppressor function to mutant p53 by a low-molecular-weight compound. Nat Med. 2002 Mar;8(3):282-8.
32. Lehmann S, Bykov VJN, Ali D, et al. Targeting p53 in vivo: A first-in-human study with p53-targeting compound APR-246 in refractory hematologic malignancies and prostate cancer. J Clin Oncol. 2012 Oct 10;30(29);3633-9.
33. Yu X, Vaxquez A, Levine AJ, Carpizo DR. Allele-specific p53 mutant reactivation. Cancer cell. 2012 May 15;21(5):614-25.
34. Yu X, Blanden AR, Narayanan S, et al. Small molecule restoration of wildtype structure and function of mutant p53 using a novel zinc-metallochaperone based mechanism. Oncotarget. 2014 Oct 15;5(19):8879-92.
35. Simabuco FM, Morale MG, Pavan ICB, et al. p53 and metabolism: from mechanism to therapeutics. Oncotarget. 2018 May 4;9(34):23780-23823.
36. Dobbin ZC, Landen CN. The Importance of the PI3K/AKT/mTOR pathway in the progress of ovarian cancer.
37. No JH, Jeon YT, Park IA, et al. Activation of mTOR signaling pathway associated with adverse prognostic factors in epithelial ovarian cancer. Gynecol Oncol. 2011 April;121(1):8-12.
38. Behbakht K, Sill MW, Darcy KM, et al. Phase II trial of the mTOR inhibitor, temsirolimus and evaluation of circulating tumor cells and tumor biomarkers in persistent and

recurrent epithelial ovarian and primary peritoneal malignancies: a Gynecologic Oncology Group study. Gynecol Oncol. 2011 Oct;123(1):19-26.
39. Strebhardt K, Ullrich A. Targeting polo-like kinase I for cancer therapy. Natl Rev Cancer. 2006. Apr;6(4):321-30.
40. Liu X, Erikson RL. Polo-like kinase (Plk) 1 depletion induces apoptosis in cancer cells. Proc Natl Acad Sci. 2003 May 13;100(10):5789-94.
41. Weichert W, Denkert C, Schmidt M, et al. Polo-like kinase isoform expression is a prognostic factor in ovarian carcinoma. Br J Cancer. 2004 Feb 23;90(4):815-21.
42. Takai N, Miyazaki T, Fujisawa K, et al. Expression of polo-like kinase in ovarian cancer is associated with histologic grade and clinical stage. Cancer Lett. 2001 Mar 10;164(1):41-9.
43. Jimeno A, Li J, Messersmith WA, et al. Phase I study of ON 01910.Na, a novel modulator of polo-like kinase 1 pathway, in adult patients with solid tumors. J Clin Oncol. 2008 Dec 1;26(34):5504-10.